

Age and Metallicity Estimation of Globular Clusters from Strömgren Photometry

Karl Rakos

Institute of Astronomy, Vienna University, Vienna, Austria; karl.rakos@chello.at

James Schombert

Department of Physics, University of Oregon, Eugene, OR; js@abyss.uoregon.edu

ABSTRACT

We present a new technique for the determination of age and metallicity in composite stellar populations using Strömgren filters. Using principal component (PC) analysis on multi-color models, we isolate the range of values necessary to uniquely determine age and metallicity effects. The technique presented herein can only be applied to old ($\tau > 3$ Gyrs) stellar systems composed of simple stellar populations, such as globular clusters and elliptical galaxies. Calibration using new photometry of 40 globular clusters with spectroscopic [Fe/H] values and main sequence fitted ages links the PC values to the Strömgren colors for an accuracy of 0.2 dex in metallicity and 0.5 Gyrs in age.

1. INTRODUCTION

The two primary processes that determine the characteristics of a stellar population are its star formation history and its chemical evolution. For an actively star forming system, such as the disk of our Galaxy, these two process are intertwined and will display a feedback loop as star formation continues and, thus, understanding an active system requires detailed HR diagrams and individual stellar spectroscopy. However, a simple stellar population (SSP), one formed in a single event from a single cloud of gas (e.g. a globular cluster), will have a fixed metallicity and age that may be derived from the color-magnitude diagram (CMD). A burst stellar population, i.e. one derived from a extended star formation event, will be composed of a combination of SSP's and the evolutionary processes are reflected into the population's age and metallicity by the luminosity weighted mean of the various SSP's. It is possible to characterize a burst population if the duration of the burst is short and distribution of metallicities is uniform (Renzini & Buzzoni 1986).

Early studies of composite stellar populations focused on broadband colors of spiral bulges and elliptical galaxies (Sandage & Visvanathan 1978, Tinsley 1980, Frogel 1985) and these datasets supported the hypothesis that red galaxies are composed, primarily, of old, metal-rich stellar populations under the burst hypothesis. Unfortunately, it was quickly realized that detailed interpretation of broadband colors with respect to age and metallicity are complicated by several factors. Foremost was the assumption that old stellar systems are composed of a uniform population in age and metallicity. It was soon demonstrated by population synthesis techniques (O'Connell 1980) that a young population quickly redden to similar integrated colors as an old population and that the change in color is abrupt even while the differences in age may be quite large (greater than 5 Gyrs). It was also noted by Burstein (1985) who found significant variations in the age and metallicity properties of galactic globular clusters which did not reflect into their integrated broadband colors. Lastly, it was identified through the use

of stellar population models that slight changes in age and metallicity operate in the same direction of spectroevolutionary parameter space (Worthey 1994). This coupling of age and metallicity (known as age-metallicity degeneracy, Worthey 1999) is due to competing contributions from main sequence turn-off stars (sensitive to age) and red giant branch (RGB) stars (sensitive to metallicity) near 5000Å. Filters that bracket this region of a galaxy’s spectrum will require increasingly accurate values for metallicity to determine a unique age and vice-versa.

To avoid the age-metallicity degeneracy problems, a majority of recent stellar population studies have focused on the determination of age and metallicity through the use of various spectral signatures, such as H β for age (Kuntscher 1998, Trager *et al.* 2001). This approach provides a finer comparison to stellar population models, but requires assumptions about the relationship between metallicity indicators (e.g. Mg₂) and the [Fe/H] value of the population as reflected into the behavior of the red giant branch. In other words, spectral lines provide the value of that element’s abundance, but what is really required is the temperature of the RGB which is a function of the total metallicity, Z . Varying ratios of individual elements to Z complicates the interpretation of line studies (Ferreras, Charlot & Silk 1999). In addition, these techniques have limitations due to the required high S/N for the data that make them problematic for the study of high redshift systems.

An alternative approach to spectral line studies is to examine the shape of specific portions of a spectral energy distribution (SED) using narrow band filters centered on regions sensitive to the mean color of the RGB (metallicity) and the main sequence turnoff point (mean age) without the overlap that degrades broadband colors. The type of galaxy examined, for example stellar systems with ongoing star formation where a mix of different age populations may be present, will still limit this technique. However, for systems that have exhausted their gas supply many Gyrs ago (i.e. old and quiescent), it may be possible to resolve the underlying population with some simple assumptions on their star formation history and subsequent chemical evolution. Thus, we have the expectation, guided by the results of evolution models, that objects composed of SSPs or a composite of SSPs (e.g. ellipticals) present special circumstances where the age-metallicity degeneracy can be resolved and allow the study of the evolution of stellar populations.

In a series of earlier papers, we have examined the uz , vz , bz , yz colors of globular clusters and used a combination of their colors and SED models to derive the mean age and metallicity of dwarf, bright and field ellipticals (Rakos *et al.* 2001, Odell, Schombert & Rakos 2002, Rakos & Schombert 2004). While spectroscopic data is superior for age and metallicity estimations in high S/N datasets, our goal has been to develop a photometric system that can be used for galaxies of low surface brightness and/or high redshift, where spectroscopy is impractical or impossible. Our past technique has been to relate the $vz - yz$ color index to mean metallicity, since the vz filter is centered on the absorption line region near 4100Å as guided by our multi-metallicity SED models. The $bz - yz$ color index, whose filters are centered on continuum regions of the spectral energy curve, measures the mean stellar age. This method was crude since metallicity changes will move the effective temperature of the RGB and, thus, the continuum $bz - yz$ colors. In our more recent work, we have included photometry through the uz filter which provides an additional handle on age and metallicity effects in the other two color indices. In addition, we have applied a principal component (PC) analysis on the multi-color data (Steindling, Brosch & Rakos 2001) that more fully isolates metallicity from age effects and the changes due to recent star formation.

The success of our narrow band, multi-color technique has motivated us to return to our original calibration objects, i.e. globular clusters, and obtain higher accuracy photometry and investigate their color behavior under PC analysis. In addition, new globular cluster age estimates are available in the literature (see Salaris & Weiss 2002), based on direct determination from the main sequence turnoff point rather than SED models, and Schulz *et al.* (2002) have published a set of new SED models for metallicities from -1.7 to $+0.4$ and ages from 10^6 yrs to 16 Gyrs using the most recent isochrones from the Padova group. Our aim for this paper is threefold: 1) to present our new photometry based on the integrated light from 40 Milky Way globular clusters with well determined ages and metallicities (baseline SSP's), 2) to demonstrate that narrow band filters are effective in discriminating age and metallicity for a single generation objects by comparison to data and SED models and 3) calibrate our photometric system to globular cluster ages and metallicities and explore its use, and limitations, as an age and metallicity estimator for dwarf and giant ellipticals.

2. DATA AND MODELS

Our primary data sample is the photometry of Milky Way globular clusters published in Rakos *et al.* (2001), with a few corrections, plus new observations obtained during the 2003 CTIO observing season. There are 40 clusters in the final sample where a small number of clusters were observed multiple times. The photometric accuracy is on the order of ± 0.02 mag in $bz - yz$ and $vz - yz$ plus ± 0.03 mag in $uz - vz$. The Strömgren filters have a long history in the literature of being used to determine metallicity, surface gravity and effective temperature in stars (Bell & Gustafsson 1978), but their use for a composite system, one composed of many stars of different luminosities and temperatures but a single metallicity, is more complicated.

Our first challenge is to demonstrate that age and metallicity in a stellar population can be discriminated solely from its narrow band colors. To this end, we first need to track the behavior of our colors by convolving our filters to a set of SED models with varying age and metallicities. Our choice of SED models is the recent work published by Schulz *et al.* (2002) which provide $uvby$ (rest frame uz, vz, bz, yz) color indices for SSP models using five different metallicities ($-1.7, -0.7, -0.4, 0.0, +0.4$) and ages between 0.8 to 14 Gyr. We have transformed these published indices to our modified system using the transformations shown in Rakos, Maindl & Schombert (1996) and applied the same PC analysis to the resulting colors as outlined in Steindling, Brosch & Rakos (2001).

Scientific data in the astronomy are usually neither linear nor orthogonal at the same time. Often, for small regions of data, linearity and orthogonality can be reached through the use of PC analysis (Murtagh & Heck 1987). Close inspection of Schulz *et al.* theoretical models has shown acceptable linearity for ages larger than 3 Gyrs over the full range of model metallicities. In this restricted region, it is possible to apply PC analysis to; 1) separate the age and the metallicity of a stellar population, 2) select the most correlated variables and 3) determine linear combinations of variables for extrapolation. In the Table 1, we list the metallicities, ages and corresponding photometric color indices ($uz - vz, bz - yz, vz - yz$) for the range of models considered herein. These correlations deliver principal components PC1, PC2 and PC3 (see Steindling, Brosch & Rakos 2001), but only first two components, PC1 and PC2, have significant content for our purpose. Their values are given by:

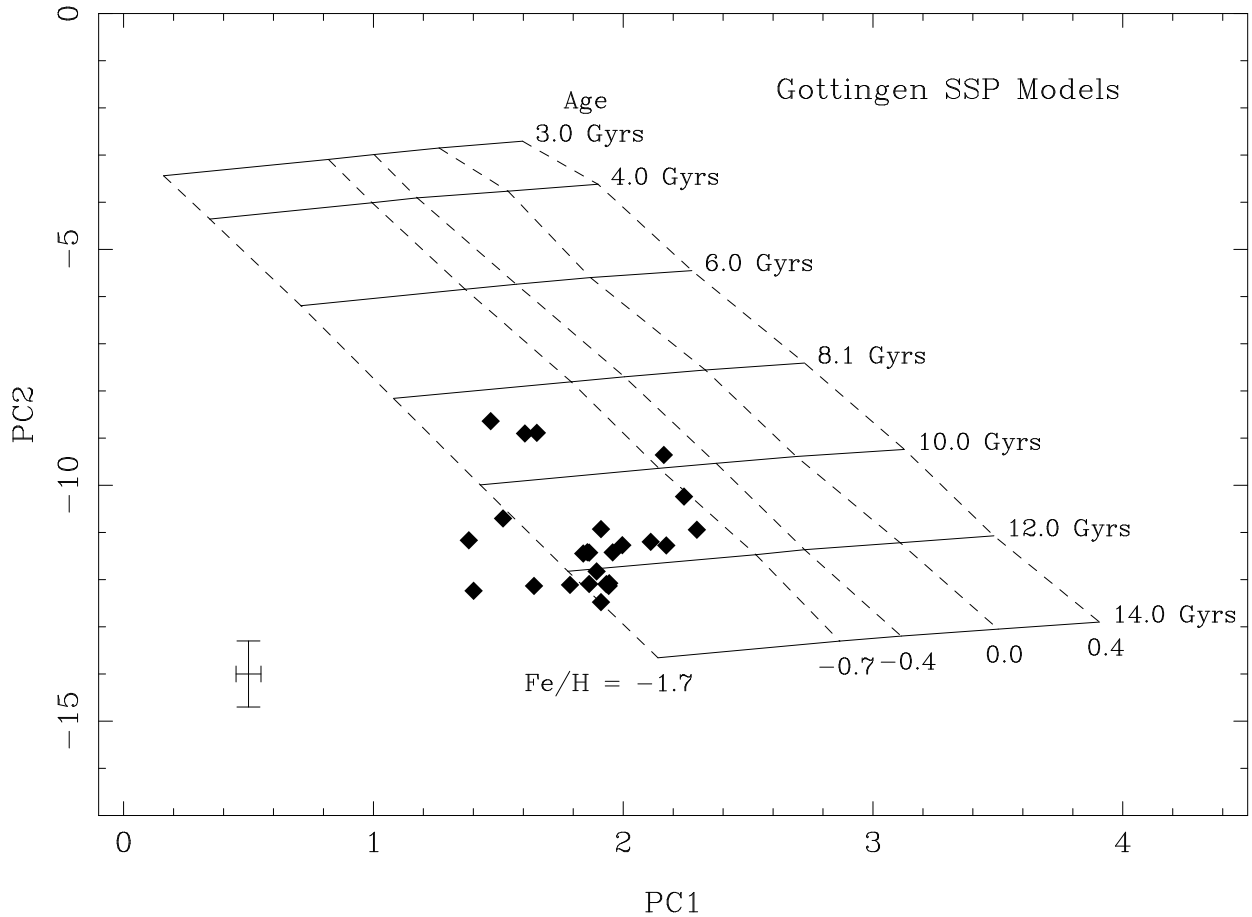


Fig. 1.— The principal component axes PC1 versus PC2 for the Schulz *et al.* SED models. Each intersection represents a single model. Age runs roughly vertical to PC1, $[\text{Fe}/\text{H}]$ runs horizontal. Globular clusters with reliable ages, metallicities and narrow band colors are shown are solid symbols (ages and metallicities from Salaris & Weiss). The error bar in the lower left-hand corner display the typical error for the Salaris & Weiss data converted to PC axis. They occupy the proper region of the grid indicating that the SED models correctly describe their color indices.

$$PC1 = 0.471[Fe/H] + 0.175\tau + 0.480(uz - vz) + 0.506(bz - yz) + 0.511(vz - yz) \quad (1)$$

$$PC2 = 0.345[Fe/H] - 0.935\tau + 0.047(uz - vz) - 0.061(bz - yz) + 0.020(vz - yz) \quad (2)$$

where τ is the age of the stellar population in Gyrs. Metallicity is found to have similar weight in both equations, contrary to the age index that has a small weight in the first equation and a large weight in the second expression. Of course, knowledge of the values for PC1 and PC2, combined with the photometric indices, would provide simple solutions to the equations for age and metallicity.

For the models in Table 1, PC1 and PC2 are calculated from equations (1) and (2) where the colors are given by the models and, of course, [Fe/H] and age are the inputs for each model. Figure 1 displays PC1 versus PC2 for a range of models and demonstrates their orthogonality between age and metallicity. We only have PC1 and PC2 model values for a few discrete values of metallicity and age, but a simple linear interpolation between these values produces PCs with significant accuracy over the entire surface in Figure 1. The advantage of the smooth behavior for age and metallicity in the PC plane is that if one has all three narrow band colors ($uz - vz$, $vz - yz$ and $bz - yz$) then knowledge of the correct PC1 and PC2 values allows for the unique determination of age and metallicity from equations (1) and (2). If the PC values are unknown, then an iterative search scheme could select a range of values for τ and [Fe/H], determine PC1 and PC2 from Figure 1, then look how well those values and the observed colors solve equations (1) and (2). We will outline this technique in greater detail in the next section.

For comparison of the models to main-sequence fitted ages and metallicities of globular clusters, we have used the results from Harris (1996, updated in February 2003) and Salaris & Weiss (2002). Salaris & Weiss provide two additional estimates for metallicity with the designation CG97 (Carretta & Gratton) and ZW84 (Zinn & West) as well as two additional estimates for ages with the same designation. We have used a mean value of all three values for the age and metallicity of each cluster (the mean error from Salaris & Weiss is ± 0.1 Gyrs in age and ± 0.1 dex in [Fe/H]) and calculated PC1 and PC2 using the observed narrow band colors and the fitted metallicities and ages. The resulting PC values are shown in Figure 1 (solid symbols) with an error bar shown in the bottom left-hand corner that represents the mean error of the Salaris & Weiss sample. The globular cluster data occupies the correct portion of the PC1-PC2 diagram and confirms that the SED models do, in fact, describe the observed colors of the globular clusters. This is not an obvious result, for previous SED models failed to match the uv colors of globular clusters by between 0.5 and 0.7 mags (Rakos *et al.* 2001). It appears that recent changes in overshoot calculations, important for the determination of colors for the blue HB stars, have converged the model colors and the observed $uz - vz$ colors of globular clusters.

3. ITERATIVE PC SOLUTIONS

Reproducing PC values for objects with known metallicities and ages only confirms the validity of the Schulz *et al.* SED models. A more powerful approach would be to derive metallicity and age values using only the observed narrow band colors and knowledge of the behavior of the PC surface (i.e.

guided by the SED models). This process begins with the production of a mesh of PC1 and PC2 values, with the expectation that one pair in the computed mesh represents the true value for an unknown age and metallicity. To identify the true value of PC1, PC2 for an object with observed colors, but unknown age and metallicity, we interpolate a pair PC1 and PC2 from the assumed age and metallicity (see Figure 1), use expressions (1) and (2) and fill in the observed color indices plus the assumed age and metallicity and compare the calculated pairs with the pairs derived from the colors.

In practice, the search for the correct age and metallicity is evaluated by calculating the differences between the PC values determined from models (i.e. Figure 1) and those PC values determined from equations (1) and (2) where the observed colors are the input. The quality of the solution is measured by the root mean difference (RMS) between the PC values over two iteration loops, one for age and one for metallicity. This computation consists of starting with a value for age and increasing the value with an index of 0.1 Gyr. Each age iteration has a nested metallicity loop increasing in steps of 0.004 dex. At each step, PC values are interpolated from the Schulz *et al.* models for the step values of age and metallicity, then compared to the PC values determined from expressions (1) and (2) again using the step values of age and metallicity plus the observed colors.

To limit interpolation errors, the starting and ending values in the first loop are fixed on values for the age of the models given by Schulz *et al.* with step values interpolated from Figure 1. Each step of the age loop has a second loop that iterates over the metallicity interval. At each step, metallicity is evaluated first using the age to calculate the metallicity from equation (1), then age is calculated from equation (2) which is then returned to equation (1), inserting the newly calculated value for age and calculating a better value for the metallicity.

Each iteration produces a better approximation for age (using equation 2) and is repeated for total of six values of age and metallicity. In the case that the iterated pair of PC1 and PC2 represents the true value, we expect it to have the smallest deviation for the calculated set of six ages and six metallicities. Therefore, we determine the quality of the solution by the sum of mean square deviations of ages and metallicities for the selected PC1 and PC2 values. While this technique is not as rigorous as a least squares minimization between two functions, it has the advantage of being a quantitative measure of the fit and the RMS sum does become smaller and smaller as we approach the proper values of age and metallicity.

Lastly, to avoid problems associated with small local minimums, we extend the search for at least four or more values of age in steps of 0.1 Gyr that have the smallest sum of mean square deviations (for a very limited range of metallicity), which implies the closest match to the proper age and the metallicity for the system. The resulting grid minimum that is searched for should be deepest and widest within the whole range of PC1, PC2 values. Unfortunately, in some cases, there is a secondary minima produced by the errors for the observed color indices and the best solution may have a broad range of age values with an equal quality of fitness. A detailed example of our procedure is given in the Appendix for globular cluster NGC 6397.

The above technique was applied to all 40 clusters with metallicity information available from spectroscopy and age dating using CMD diagrams. For one cluster, NGC 6218, no acceptable solution was found, the rest are listed in Table 2 where $\langle \text{Fe}/\text{H} \rangle$ and $\langle \tau \rangle$ are the values from Salaris & Weiss and $[\text{Fe}/\text{H}]_{ph}$ and τ_{ph} the photometric determination of metallicity and age. A comparison of these

two determinations are shown in Figures 2 and 3 where the solid blue lines represent a one-to-one relationship between $\langle \text{Fe}/\text{H} \rangle$, $\langle \tau \rangle$ and the photometrically determined $[\text{Fe}/\text{H}]_{ph}$, τ_{ph} . The solid black lines are a least squares fit to the relationships. Both relationships are well within the internal errors for metallicity and age from main sequence fitting as will be discussed in the next section.

4. UNCERTAINTIES AND ERROR ESTIMATES

The uncertainties to our technique fall into three categories; 1) observational errors to the colors, 2) errors due to the quality of the solutions from the iterative method, i.e. the range of equally likely solutions based on a quality of fit criteria and 3) the ability of the Schulz *et al.* models to reproduce the underlying physical reality to the globular cluster colors. While we can directly test the impact of errors for the first two quantities, we cannot address the meaning of the fits in terms of the various inputs to the population models. However, we can compare our technique results with the age and metallicities determined by other means, in this case by comparing to the results from CMD fitting and spectroscopy, as an indication of the merit of the models as applied to our method.

Observational error can arise through inaccuracy to the photometry either through simple Poisson noise on the photon counts or internal errors to the standard stars or uncertain Galactic reddening values. As described in the previous sections, the data was obtained under the best of conditions and the error is estimated to be 0.02 for $bz - yz$ and $vz - yz$ and 0.03 for $uz - vz$. In order to estimate the effect of this error on the age and metallicity determination, we have simply iterated the solution technique using a range of colors within the measured errors. Uncorrelated errors (i.e. randomly changing each color by its mean error) produces solutions that varied by ± 0.5 Gyrs in age and ± 0.05 dex in $[\text{Fe}/\text{H}]$. Correlated errors, for example moving all the colors to the blue, produced similar errors since bluer $uv - vz$ colors increase age and metallicity fits whereas bluer $vz - yz$ and $bz - yz$ colors decreased the fits.

Another source of uncertainty arises from the ability to determine a unique solution to the given narrow band colors. This, in effect, asks if the resulting PC pairs can produce a unique set of age and metallicity values within a certain degree of accuracy. One method of estimating the quality of the solutions is to examine the behavior of the fits for a range of age and metallicities near the chosen solution. For our technique, this involves comparing the RMS values for each of the nested loops. The loops with the smallest deviations from the mean are the ones closest to the derived solution (see the Appendix for an example of this using cluster NGC 6397).

The goodness of fit criteria assumes that age and metallicity are uncorrelated, which we know to be false. However, as an iterative procedure, we can test each age and metallicity loop separately and find a solution that converges in both parameters. An example of the RMS space for NGC 1904 is shown in Figure 4. Each contour represents a normalized sum of the RMS values for the age and metallicity loops per PC pair (in this example, age was iterated by 0.1 Gyrs and $[\text{Fe}/\text{H}]$ by 0.005 dex). A minimum is found at accepted solution of 11.9 Gyrs and $[\text{Fe}/\text{H}] = -1.55$ with a secondary minimum at 11.6 Gyrs. While secondary minimum are common in the sample, they were always located with 0.5 Gyrs of the primary minimum, i.e. within the errors as given by observational error on the colors. Also of interest is the direction of the ‘valley’ of low RMS which tracks from high metallicity, younger

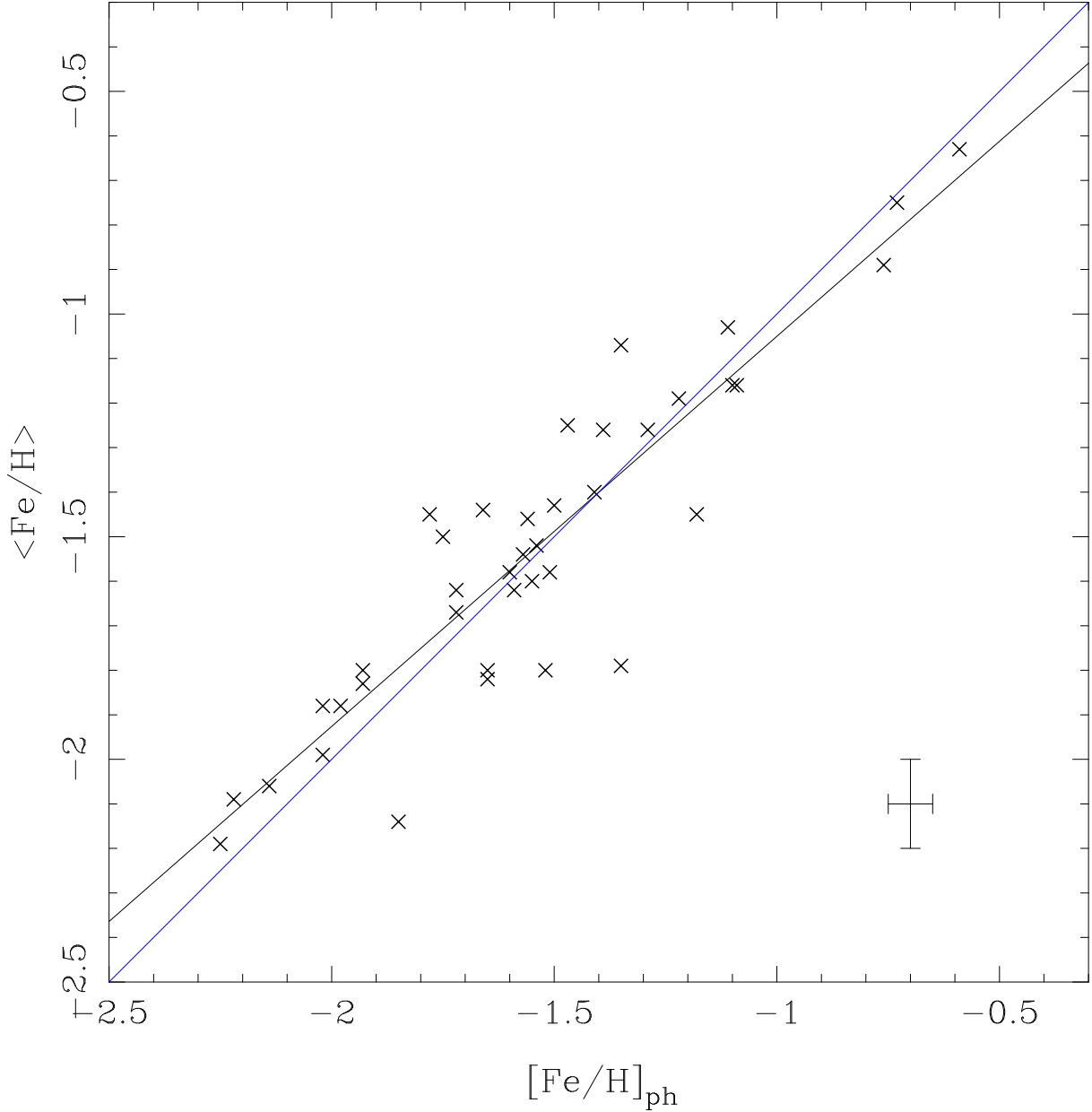


Fig. 2.— The globular cluster metallicities as determined by the iterative technique ($[\text{Fe}/\text{H}]_{\text{ph}}$) versus their true metallicity ($\langle \text{Fe}/\text{H} \rangle$, a mean value from the literature). The blue line indicates a one-to-one relationship, the black line is a least square fit. The error bar displays the typical uncertainty in metallicity from Salaris & Weiss as well as the uncertainty in our fitting technique.

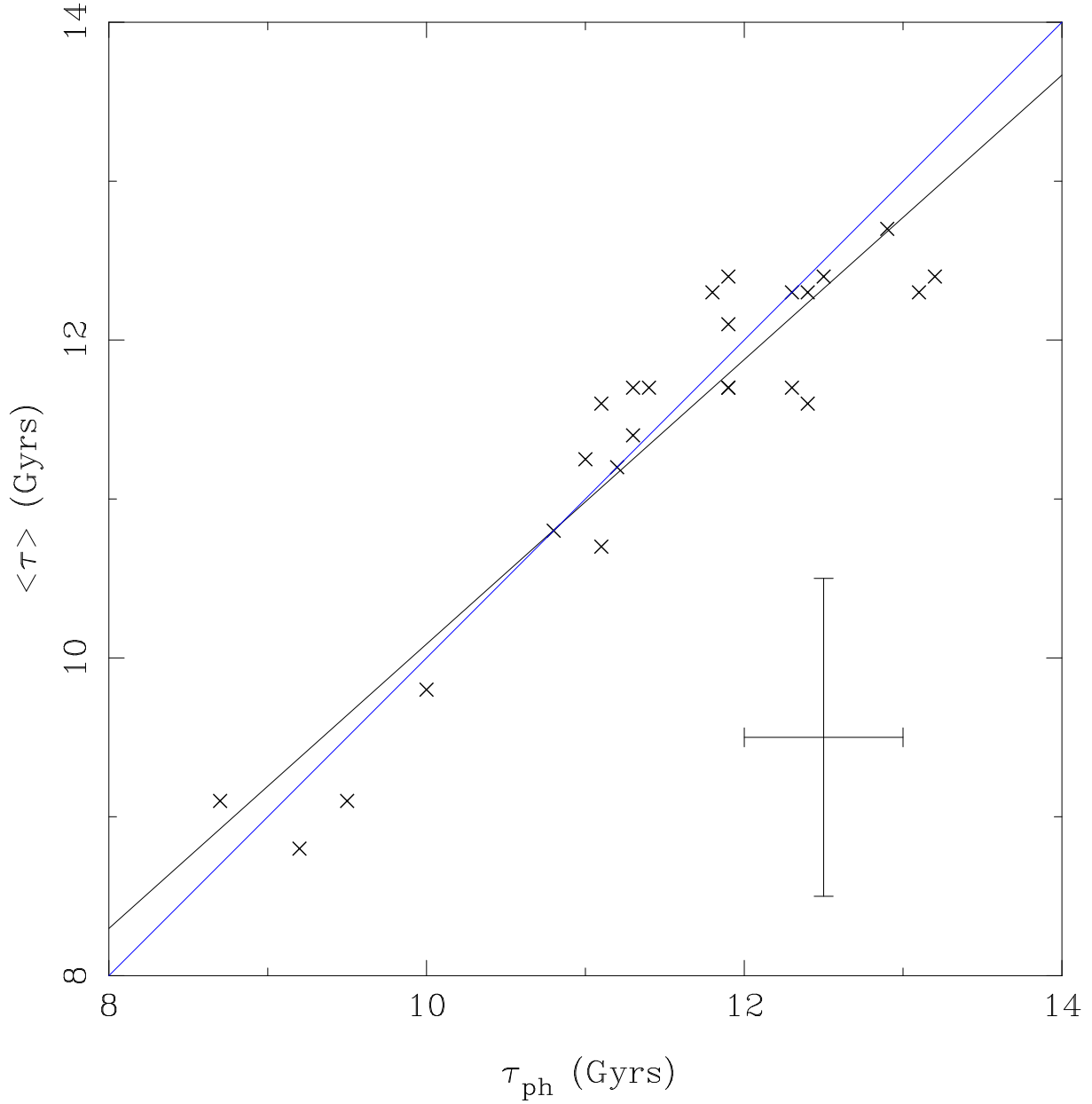


Fig. 3.— The globular cluster ages as determined by the iterative technique (τ_{ph}) versus their true age from main sequence fitting ($\langle\tau\rangle$, a mean value from the literature). The blue line indicates a one-to-one relationship, the black line is a least square fit. The error bar displays the typical uncertainty in age from Salaris & Weiss as well as the uncertainty in our fitting technique.

age to lower metallicities, older age. This is the age-metallicity degeneracy and the slope of the ‘valley’ is $\delta \log(\text{age})/\delta(Z) = -1$ as predicted by Worthey (1999) for a near-blue filter system. The difference here is that a clear minimum can be determined (and the full range given by the Schulz *et al.* models are searched), although any error in either age or metallicity will reflect into the other with the slope given above (i.e. along the ‘valley’).

Inspection of the example in the Appendix demonstrates that the RMS minimum are shallower for age loops compared to metallicity loops. This confirms that our chosen filter system is more sensitive to metallicity than age and, therefore, the uncertainty associated with age will be greater than that of metallicity. Examination of the RMS contours of the globular clusters in the sample finds that the formal errors on the solutions are 0.4 Gyrs in age and 0.01 dex in [Fe/H], which is less than the error expected from observational uncertainties. Hence, we conclude that the fitting process does not represent the dominant source of uncertainty to our method and that the age-metallicity degeneracy is broken within the accuracy of the data. We note, however, the range of models we use to construct the PC pairs limits this statement. In particular, we do not examine models with ages less than 3 Gyrs as these represent unrealistic ages when considering old stellar populations. Thus, age-metallicity degeneracy may once again come into play for very young populations or ones with super-solar metallicities and we stress this caveat in any future usage of this technique.

To evaluate the accuracy of the entire technique, including the ability of the Schulz *et al.* models to reproduce the integrated colors of globular clusters, we return to Figures 2 and 3, the comparison between the PC solutions and the values for age and metallicity as determined by CMD fitting from Salaris & Weiss (2002). Representative error bars are shown in the bottom right hand portion of each diagram. The error in the y-axis is taken from the mean error in Salaris & Weiss. The error in the x-axis represents the values for the limits on our technique discussed above. Both age and metallicity are recovered through the narrow band colors using our PC technique and the difference from the one-to-one line and a least-squares fit is negligible. Since the formal error for our solutions is less than the error associated with CMD dating, it is tempting to claim that integrated colors are better predictors of age and metallicity. However, it is more likely that the interplay between the data in CMD’s for globular clusters and stellar evolutionary models is also present in our technique and the Schulz *et al.* SSP models. Thus, we adopt the scatter in Figures 2 and 3 as the real uncertainty to our technique. In Figure 2, the scatter around mean metallicity is approximately 0.2 dex, greater than the internal error to our technique or the calibrating cluster metallicities. In Figure 3, the scatter around mean age is 0.5 Gyrs limited by the calibrating age from CMD fits that have an error of ± 1 Gyr. This appears to be an accuracy limit for globular clusters (probably any type of SSP) until a set of better determined ages is found to test against our method.

5. METALLICITY CALIBRATION

In a previous paper (Rakos *et al.* 2001), we have demonstrated a very tight correlation between $vz - yz$ color and the published metallicities for globular clusters deriving the relation:

$$[\text{Fe}/\text{H}] = (2.57 \pm 0.13)(vz - yz) - (2.20 \pm 0.04) \quad (3)$$

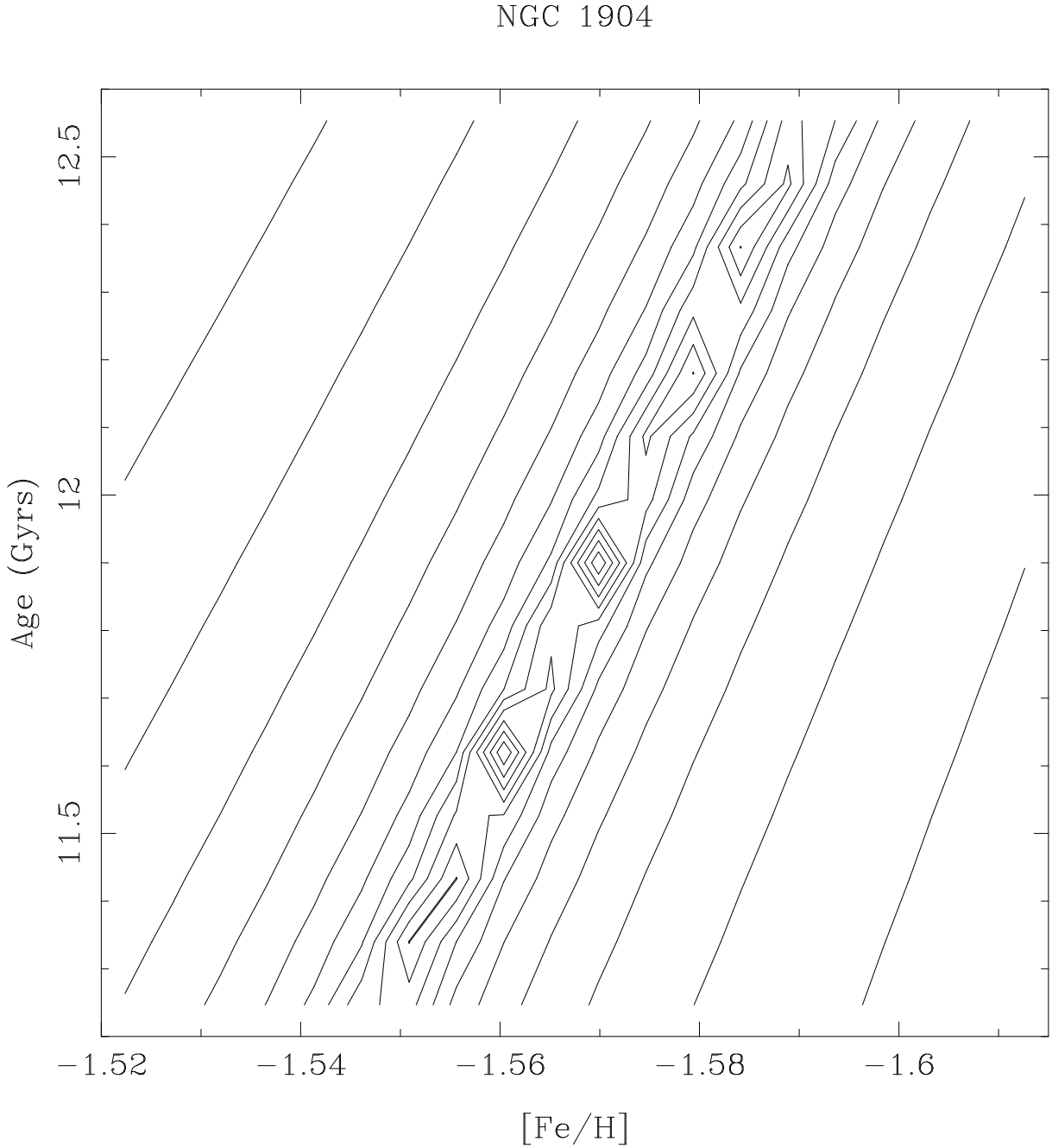


Fig. 4.— The RMS contours of the iterative solutions for the cluster NGC 1904. The lowest contour represents an RMS of 0.001, increasing by a factor of three each contour. The primary minimum is found at 11.9 Gyrs and $[\text{Fe}/\text{H}] = -1.55$ with a secondary minimum at 11.6 Gyrs. No other minimums were found in the parameter space given by the Schulz *et al.* models (although note that we only consider models older than 3 Gyrs).

where the scatter of individual values corresponds to the probable errors published in the literature. Examining the relation (1) for principal components, we find, as expected, that the calculated metallicity value will be influenced, in a lesser manner, by the other two color indices. From an analysis of computed $[\text{Fe}/\text{H}]$ values ($[\text{Fe}/\text{H}]_{ph}$, see Table 2), we find a very similar expression (see Figure 5):

$$[\text{Fe}/\text{H}]_{ph} = (3.034 \pm 0.177)(vz - yz) - (2.305 \pm 0.049) \quad (4)$$

Note that the fairly good correlation between $vz - yz$ and metallicity is due to the small value for the coefficient of age in equation (1) plus the fact that the globular clusters used herein have a small range of age (8 to 13 Gyrs). Thus, this ‘fast’ calibration from color to $[\text{Fe}/\text{H}]$ is only relevant for old stellar populations. Also shown in Figure 5 is the relationship for $bz - yz$, which is clearly not linear but does follow the predicted trend of bluer continuum colors for lower metallicity clusters. Since the calculated $[\text{Fe}/\text{H}]_{ph}$ values are related to the real metallicity values (see Figure 2) by the following linear regression:

$$\langle \text{Fe}/\text{H} \rangle = (0.876 \pm 0.065)[\text{Fe}/\text{H}]_{ph} - (0.174 \pm 0.104) \quad (5)$$

where $\langle \text{Fe}/\text{H} \rangle$ is mean value of $[\text{Fe}/\text{H}]$ from Salaris & Weiss. Substituting for $[\text{Fe}/\text{H}]_{ph}$ gives:

$$\langle \text{Fe}/\text{H} \rangle = (2.658 \pm 0.089)(vz - yz) - (2.193 \pm 0.052) \quad (6)$$

which is nearly identical to equation (3). We can use this solution as a quick estimation of metallicity with the knowledge of only one color index, $vz - yz$, since $vz - yz$ is the most sensitive indicator of metallicity due to its measurement of an absorption line rich region of the spectrum. To achieve a more accurate estimate of metal abundance, we would need the mean effective temperature of the stellar population in order to calculate the abundance directly from the strength of absorption lines. This implies that the relationship between $vz - yz$ is only true for the systems composed of stellar populations of identical temperatures. Therefore, in the absence of temperature information, we combine all three colors as given by PC1 resulting in:

$$X = 0.480(uz - vz) + 0.506(bz - yz) + 0.511(vz - yz) \quad (7)$$

and derive the approximation

$$[\text{Fe}/\text{H}] = -4.24 + 6.47X - 2.29X^2 \quad (8)$$

which is plotted in Figure 6 for visual comparison. This relation delivers the same values for the metallicity as the principal component analysis for globular clusters and SSP models. In addition, we can apply the same PC method outlined above on the multi-color data we have acquired for dwarf and bright ellipticals from our Coma and field samples (Odell, Schombert & Rakos 2002). The resulting $[\text{Fe}/\text{H}]$ values for this sample of galaxies are also shown in Figure 6, with the caveat here being that the galaxies are assumed to be SSP’s like globular clusters. While galaxies follow the same trend as

globulars in Figure 6, the relationship is not linear. We interpret this as confirmation that ellipticals are not SSP’s, but rather the summation of many SSP’s to form a composite stellar population. However, the low order difference between globulars and ellipticals signals that the SSP assumption is an adequate approximation for many needs and that the total stellar population in ellipticals must be a simple form (such as a gaussian distribution) to produce the correlation seen in Figure 6 (see also Smolcic *et al.* 2004). In fact, a simple 2nd order function can be fit to both the globular cluster and elliptical data in Figure 6 (shown as the solid line) that empirically can be used to determine the mean metallicity over 6 orders of magnitude in stellar mass.

6. AGE CALIBRATION

Unfortunately, there is no similar simple solution for the estimation of age as there was for metallicity. In general, mean stellar age is correlated with metallicity since an older population formed from low metallicity material, but this correlation is rather variable as effected by the local environment and the local history of star formation. And, of course, this is the parameter we wish to determine in order to understand the galaxy evolution process. Globular clusters in our Galaxy display such a difference between younger and older clusters as divided by age on the order of 10 Gyrs where older clusters are more metal-poor.

The computed ages for measured globular clusters are listed in Table 2. The recent compilation and discussion of globular ages is found in Salaris & Weiss (2002). There are two sets of ages with designation CG97 and ZW84 and, again, the mean is compared with our measurements listed as τ_{ph} in Figure 3. The correlation is better than expected and comparable to the correlation between CG97 and ZW84 itself. For comparison, we have at our disposal only 26 values from the paper of Salaris & Weiss against our 40 photometric measurements. We can calculate the mean value of square differences between our estimation and the mean age of CG97 and ZW84, and these are plotted in Figure 7. The scatter increases toward larger ages or for metallicities below -1.7 . This implies a higher uncertainty for values extrapolated outside the models we have used. The realistic estimations of stellar population ages are, until now, very scarce and, outside our Galaxy, practically impossible unless the underlying HR diagram can be resolved (see Grebel 2004).

An alternative approach would be to derive the metallicity of an object as shown in the previous section, then apply a linear combination of $[\text{Fe}/\text{H}]$ and all three narrow band colors. For the globular cluster sample, this is shown in Figure 8, again using the PC values from equation (2). The resulting correlation is poor, although a least squares linear fit can be made and is shown in Figure 8. Much of the power in the fit is due to that fact that the globular cluster sample has a fair correlation between metallicity and age, however, the relative differences in age can be derived and the method shows promise as a method to separate old and young galaxies in a relative sense, which can be a key test to hierarchical models of galaxy formation (Rakos & Schombert 2004).

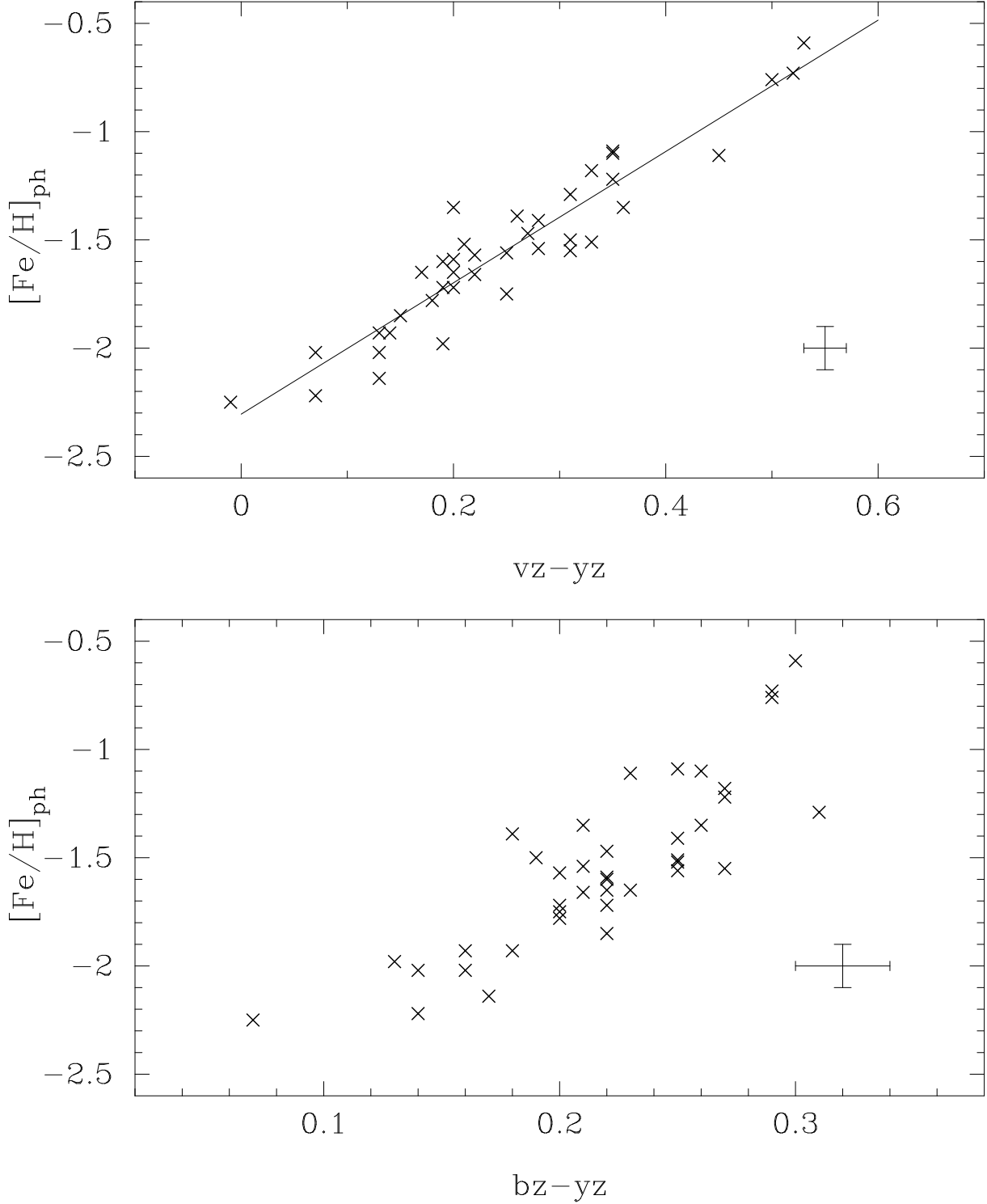


Fig. 5.— The globular cluster $vz - yz$ and $bz - yz$ colors as a function of the calculated $[Fe/H]_{ph}$. The metallicity color, $vz - yz$, displays better linearity and lower scatter than the continuum color, $bz - yz$. An adequate measure of $[Fe/H]$ can be obtained simply from the $vz - yz$ color, if the population is older than 3 Gyrs. The solid line is a least squares fit to the $vz - yz$ data as quoted in the text.

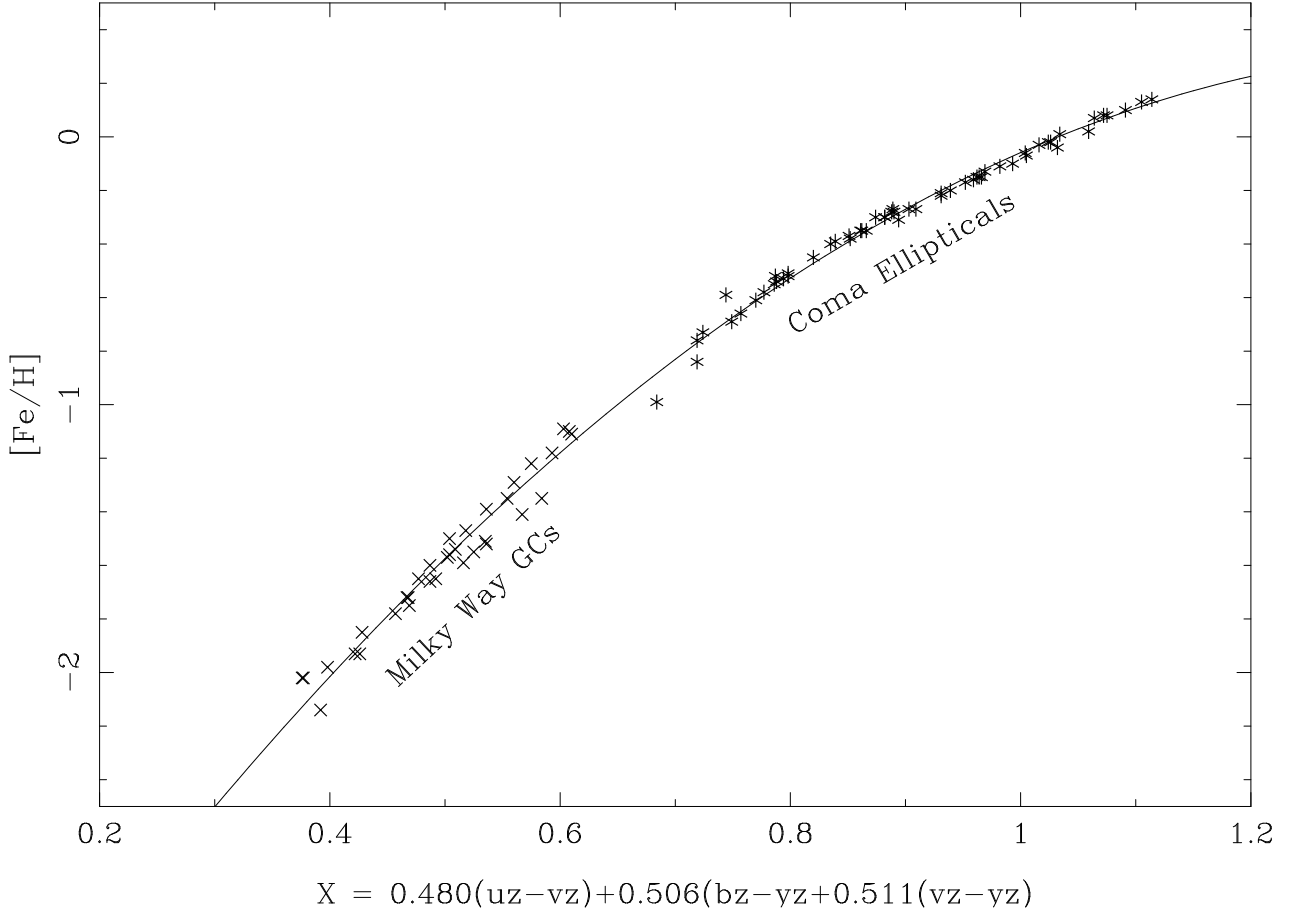


Fig. 6.— The mean metallicity of the globular cluster sample as determined by the iterative technique versus the multi-color term that incorporates all of the PC terms. This relationship can be compared to Figure 5 to demonstrate how the use of the full parameter space reduces the scatter in [Fe/H]. Also shown are the iterative results for a sample of dwarf and giant ellipticals in the Coma cluster with full *uvby* photometry. The relationship become less linear for galaxies due to the fact that they are composed of a integrated population of SSP's. The low scatter indicates that metallicity is the primary driver of galaxy color (see also Smolcic *et al.* 2004).

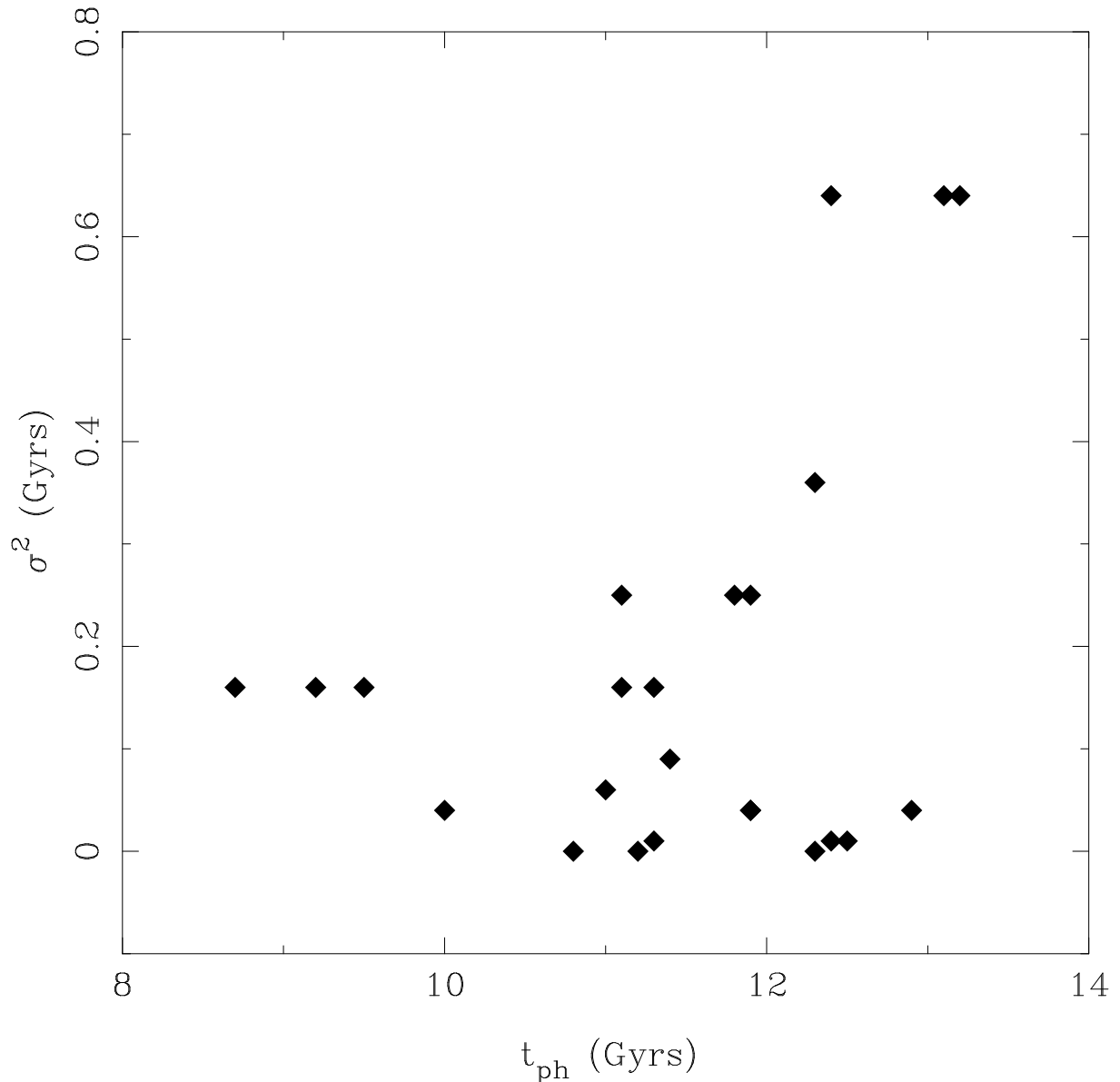


Fig. 7.— The square of the differences between our iterative estimate of cluster age and the true cluster age versus the calculated age, τ_{ph} . The difference increases with decreasing age (and decreasing metallicity) implying higher uncertainty as one extrapolates outside the model realm.

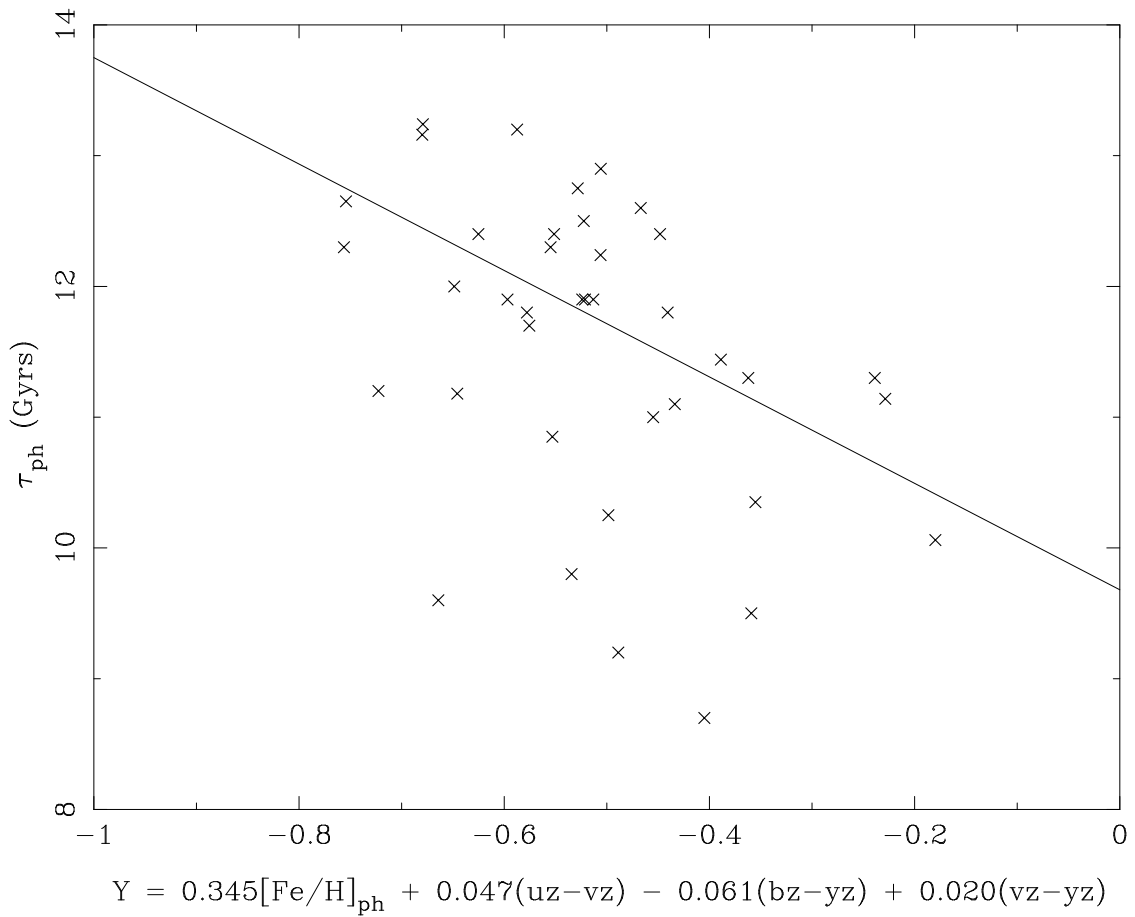


Fig. 8.— The calculated cluster age, τ_{ph} , by the iterative technique as a function of the PC2 indices including [Fe/H]. While the correlation is not as clear as the metallicity relationship, the general trend is discernible and will serve as a crude indicator of age for more complex systems.

7. SUMMARY

In this paper we have revised the age and metallicity calibration for the Strömgren filter system as applied to globular clusters and elliptical galaxies. We have first investigated the behavior of the color indices using the most recent SED models (Schulz *et al.* 2002) and applied a principal component (PC) analysis on the SED models to determine the PC axis as well as the range and limitations of the color system. With this information, we have developed a technique to derive age and metallicity for a simple stellar population by an iterative calculation scheme. To test this method, we have obtained new photometry of 40 globular clusters with well-determined age and metallicity values and demonstrated that we can recover their star formation history values using our iterative scheme. Lastly, we have re-determined the age and metallicity calibration for galaxies with new multi-color indices and tested the calibration against a sample of field and cluster ellipticals that contain a variety of spectroscopic and photometrically determined stellar population indicators.

Our next paper will be concentrate on the application of our method on dwarf and normal ellipticals in clusters of galaxies. However, we can already deduce from the low scatter in [Fe/H] curves that the observed colors in ellipticals are primarily driven by metallicity, and not age, effects. While absolute age determination is problematic, relative age measurements on the level of 1 Gyr can be extracted with sufficiently accurate photometry (errors less than 0.02 mags).

A. APPENDIX

As an example to our technique to derive metallicity and age from the PC components of a SSP, we demonstrate the calculation procedure for the globular cluster NGC 6397. We have selected NGC 6397 as an example since its [Fe/H] value (-1.88) is lower than the range of model values and, thus, we must use an extrapolation allowing the metallicity loop to run over the border given by the lowest model metallicity (-1.7). Equation (6) gives an initial estimate for the metallicity of NGC 6397 of $[\text{Fe}/\text{H}] = -2.01$, equation (8) predicts -2.13 .

In Table 3, three pairs of age (12.4, 13.5 and 13.9 Gyrs) and metallicity (-1.966 , -1.978 and -2.206) are selected to cover a broad range of age and metallicity at the boundary of the published models. Six of the iterated test values using equations (1) and (2) are shown below each pair. As each test converges on a unique PC1 and PC2 value, the range in age and metallicity values becomes smaller. This is measured by the mean values of each loop and the sum of the squares of the deviations from mean. For the initial loop, these deviations are large, as expected. From further iterations we find the minimum to be between the first two pairs.

Table 4 displays six more pairs for ages from 12.9 to 13.4 Gyr and metallicities from -2.014 to -2.034 . The top portion of the table displays the age results for six iterative searches (metallicity loops are not shown). There is little variation in age within each loop represented by a nearly constant value for the sum of the squares of the deviations from mean indicating a broad range of acceptable solutions for age. Below the age loop values is a single sequence of metallicity loops (age loop no. 4 in this case, although the variation from loop to loop was small). In the metallicity loop there is a detectable trend in the sum of the deviations. We can plot the selected pair values as a function of sum of the squares of the deviations for the metallicity (Figure 9) to demonstrate the final result, a parabola with a clear

minimum that displays probable errors of about ± 0.03 dex in metallicity and ± 0.2 Gyr in age.

While the solutions are older in age and lower in metallicity than the CMD fits from Salaris & Weiss, this cluster is an extreme example and outside the models shown in Figure 1, yet still converges to a solution. In addition, we note that Pasquini *et al.* (2004) find an age for NGC 6397 that is 0.3 Gyrs older than the Galactic disk based on beryllium measurements. Strömgren photometry of the Galactic disk derives an estimate for its age between 13.2 and 13.5 Gyrs (Twarog 1980), which would make our age determination of 13.2 Gyrs for NGC 6397 exactly in line with the beryllium value.

The authors wish to thank the directors and staff of CTIO for granting time for this project. Financial support from Austrian Fonds zur Foerderung der Wissenschaftlichen Forschung and NSF AST-0307508 is gratefully acknowledged. We also wish to thank the referee, James Rose, for his excellent suggestions to improve the presentation of our technique.

REFERENCES

Bell, R. & Gustafsson, B. 1978, A&AS34, 229

Burstein, D. 1985, PASP, 97, 89

Ferreras, I., Charlot, S. & Silk, J. 1999, ApJ, 521, 81

Frogel, J. 1985, ApJ, 298, 528

Grebel, E. 2004, Carnegie Observatories Astrophysics Series, Vol 4: Origin and Evolution of the Elements, ed. A. McWilliam and M. Rauch (Cambridge: Cambridge Univ. Press), p. 237

Harris, W. 1996, AJ, 112, 1487

Murtagh, F. & Heck, A. 1987, Multivariate Data Analysis in Astroph. and Space Science Library, D.Reidel Publ. Comp. the Kluwer A. Publishers Group.

O'Connell, R. 1980, ApJ, 236, 430

Odell, A., Schombert, J. & Rakos, K. 2002, AJ, 124, 3061

Pasquini, L., Bonifacio, P., Randich, S., Galli, D. & Gratton, R. 2004, A&A, 426, 651

Rakos, K., Maindl, T. & Schombert, J. 1996, ApJ, 466, 122

Rakos, K., Schombert, J., Maitzen, H., Prugovecki, S. & Odell, A. 2001, AJ, 121, 1974

Renzini, A. & Buzzoni, A. 1986, Spectral Evolution of Galaxies, eds. C. Chiosi and A. Renzini (Dordrecht: Reidel), p. 195

Sandage, A. & Visvanathan, N. 1978, ApJ, 223, 707

Salaris, M. & Weiss, A. 2002, å388, 492

Schulz, J., Fritze-v, Alvensleben,, Moumller, C. & Fricke, K. 2002, A&AS, 392, 1

Smolcic, V., Ivezic, Z., Gacesa, M., Rakos, K., Pavlovski, K., Ilijic, S., Lupton, R., Schlegel, D., Kauffmann, G., Tremonti, C., Brinchmann, J., Charlot, S., Heckman, T., Knapp, G. & Gunn, J. 2004, MNRAS, in press

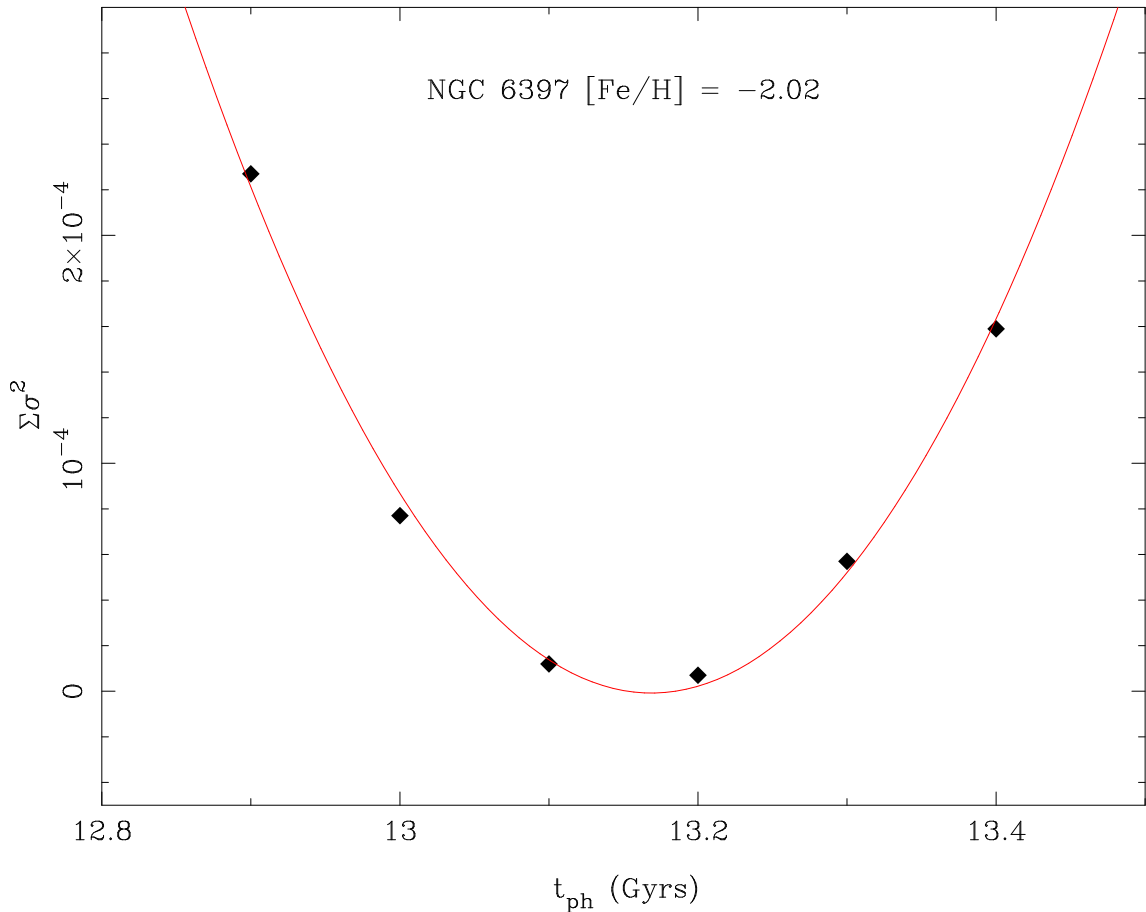


Fig. 9.— A visual example of the iterative difference errors for six [Fe/H] values in the globular cluster NGC 6397 data (see Table 4) where the sum of the squares of the deviations from the mean is plotted versus the iteration pairs of age and metallicity. The solid line is a 2nd order fit to the errors displaying a clear minimum at age/metallicity pair 13.2 Gyrs and [Fe/H]=−2.026.

Steindling, S., Brosch, N. & Rakos, K. 2001, ApJS, 132, 19
Tinsley, B. 1980, Fund. of Cosmic Physics, Vol. 5, p. 287
Twarog, B. 1980, ApJ, 242, 24
Worley, G. 1994, ApJS, 95, 107
Worley, G. 1999, ASP Conference Proceedings, Vol. 192, p. 283

Table 1. SED Models

PC1	PC2	[Fe/H]	τ^a	$uz - vz$	$bz - yz$	$vz - yz$
0.160	-3.439	-1.7	3.08	0.725	0.117	0.028
0.345	-4.357	-1.7	4.06	0.691	0.137	0.066
0.710	-6.193	-1.7	6.02	0.646	0.167	0.123
1.080	-8.158	-1.7	8.12	0.620	0.179	0.140
1.428	-9.992	-1.7	10.08	0.599	0.190	0.159
1.779	-11.824	-1.7	12.04	0.606	0.192	0.165
2.139	-13.656	-1.7	14.00	0.623	0.199	0.177
0.820	-3.094	-0.7	3.08	0.719	0.212	0.309
0.995	-4.011	-0.7	4.06	0.716	0.215	0.317
1.367	-5.844	-0.7	6.02	0.713	0.232	0.360
1.792	-7.807	-0.7	8.12	0.727	0.258	0.432
2.143	-9.639	-0.7	10.08	0.731	0.260	0.442
2.531	-11.470	-0.7	12.04	0.760	0.275	0.489
2.867	-13.303	-0.7	14.00	0.759	0.272	0.479
1.003	-2.990	-0.4	3.08	0.739	0.230	0.354
1.175	-3.907	-0.4	4.06	0.718	0.231	0.375
1.572	-5.739	-0.4	6.02	0.731	0.256	0.443
2.005	-7.701	-0.4	8.12	0.768	0.279	0.513
2.372	-9.533	-0.4	10.08	0.785	0.287	0.537
2.726	-11.364	-0.4	12.04	0.801	0.288	0.543
3.113	-13.196	-0.4	14.00	0.829	0.303	0.587
1.263	-2.851	0.0	3.08	0.745	0.257	0.463
1.539	-3.765	0.0	4.06	0.805	0.293	0.576
1.869	-5.598	0.0	6.02	0.784	0.291	0.571
2.329	-7.557	0.0	8.12	0.872	0.312	0.648
2.693	-9.389	0.0	10.08	0.886	0.320	0.669
3.109	-11.219	0.0	12.04	0.945	0.340	0.736
3.501	-13.049	0.0	14.00	0.996	0.349	0.776
1.597	-2.707	0.4	3.08	0.865	0.289	0.604
1.899	-3.619	0.4	4.06	0.949	0.332	0.737
2.275	-5.449	0.4	6.02	1.010	0.333	0.743
2.726	-7.409	0.4	8.12	1.062	0.356	0.836
3.126	-9.240	0.4	10.08	1.108	0.375	0.884
3.484	-11.071	0.4	12.04	1.130	0.375	0.894
3.907	-12.900	0.4	14.00	1.212	0.392	0.955

Note. — ^a Age in Gyrs

Table 2. Globular Cluster Data

NGC	$uz - vz$	$bz - yz$	$vz - yz$	E(B-V)	[Fe/H] ^a	τ^b	[Fe/H] _{ph}	τ_{ph}^c
104	0.65	0.29	0.52	0.04	-0.75	10.7	-0.73	11.1
288	0.51	0.31	0.31	0.03	-1.26	11.6	-1.29	11.1
362	0.54	0.27	0.35	0.05	-1.19	9.1	-1.22	8.7
1261	0.56	0.22	0.27	0.01	-1.25	8.8	-1.47	9.2
1851	0.62	0.26	0.35	0.02	-1.16	9.1	-1.10	9.5
1904	0.60	0.20	0.22	0.01	-1.54	12.1	-1.57	11.9
2298	0.63	0.25	0.21	0.14	-1.80	12.7	-1.52	12.9
3201	0.60	0.27	0.33	0.23	-1.45	11.7	-1.18	11.4
4147	0.58	0.16	0.13	0.02	-1.83	–	-1.93	11.2
4372	0.40	0.14	0.07	0.39	-2.09	–	-2.22	12.7
4590	0.50	0.17	0.13	0.05	-2.06	11.2	-2.14	11.2
4833	0.54	0.18	0.14	0.32	-1.80	–	-1.93	12.0
5024	0.50	0.14	0.13	0.02	-1.99	–	-2.02	13.2
5139	0.53	0.22	0.20	0.12	-1.62	–	-1.72	11.8
5272	0.54	0.21	0.28	0.01	-1.52	11.7	-1.54	11.9
5286	0.56	0.20	0.19	0.24	-1.67	–	-1.72	11.7
5466	0.52	0.07	-0.01	0.00	-2.19	12.3	-2.25	12.3
5634	0.49	0.13	0.19	0.05	-1.88	–	-1.98	9.6
5897	0.58	0.22	0.20	0.09	-1.82	12.3	-1.65	12.4
5904	0.65	0.18	0.26	0.03	-1.26	11.3	-1.39	11.0
5986	0.58	0.22	0.19	0.28	-1.58	–	-1.60	9.8
6101	0.57	0.23	0.17	0.05	-1.80	10.8	-1.65	10.9
6171	0.55	0.23	0.45	0.33	-1.03	11.7	-1.11	11.3
6205	0.50	0.20	0.25	0.02	-1.50	12.4	-1.75	13.2
6218	0.44	0.17	0.28	0.19	–	12.6	–	–
6229	0.52	0.19	0.31	0.01	-1.43	–	-1.50	10.3
6352	0.67	0.30	0.53	0.21	-0.63	9.8	-0.59	10.1
6397	0.54	0.16	0.07	0.18	-1.88	12.3	-2.02	13.2
6584	0.56	0.21	0.22	0.10	-1.44	11.7	-1.66	12.3
6652	0.66	0.29	0.50	0.09	-0.89	11.4	-0.76	11.3
6656	0.48	0.27	0.31	0.34	-1.60	12.4	-1.55	12.5
6681	0.52	0.25	0.25	0.07	-1.46	11.7	-1.56	11.9
6715	0.50	0.25	0.33	0.15	-1.58	–	-1.51	12.2
6723	0.56	0.26	0.36	0.05	-1.07	11.6	-1.35	12.4
6752	0.55	0.20	0.18	0.04	-1.45	12.4	-1.78	11.9
6809	0.72	0.21	0.20	0.08	-1.79	12.3	-1.35	11.8
6864	0.62	0.25	0.35	0.16	-1.16	–	-1.09	10.4
6981	0.62	0.25	0.28	0.05	-1.40	–	-1.41	12.6
7078	0.50	0.22	0.15	0.10	-2.14	–	-1.85	12.4
7089	0.63	0.22	0.20	0.06	-1.62	–	-1.59	12.8

Note. — ^a Mean value from Harris (1996) and Salaris & Weiss (2002) ^b Salaris & Weiss (2002), age in Gyrs ^c Age in Gyrs

Table 3. NGC 6397 Initial Loop

Age (Gyrs)/[Fe/H]	12.4/−1.966	13.5/−1.978	13.9/−2.206
Test no:	12.42/−1.944	13.53/−1.935	13.88/−2.322
2	12.45/−1.904	13.57/−1.861	13.84/−2.528
3	12.49/−1.834	13.63/−1.733	13.75/−2.905
4	12.54/−1.713	13.71/−1.713	13.57/−3.626
5	12.62/−1.504	13.85/−1.163	13.19/−5.123
6	12.75/−1.155	14.05/−0.601	12.31/−8.850
Mean	12.54/−1.676	13.72/−1.469	13.42/−4.226
Sum σ^2	0.075/0.4512	0.193/1.2900	1.804/30.799

Table 4. NGC 6397 Age/[Fe/H] Loops

Selected Age and [Fe/H]	12.9/ −2.014	13.0/ −2.018	13.1/ −2.022	13.2/ −2.026	13.3/ −2.030	13.4/ −2.034
Age Loop no:	12.92	13.02	13.12	13.22	13.32	13.42
2	12.93	13.04	13.14	13.24	13.34	13.44
3	12.95	13.05	13.15	13.25	13.35	13.45
4	12.97	13.07	13.17	13.27	13.37	13.47
5	12.99	13.09	13.19	13.29	13.39	13.49
6	13.01	13.11	13.21	13.31	13.41	13.51
Mean	12.96	13.06	13.16	13.26	13.36	13.46
Sum σ^2 ($\times 10^{-4}$)	61	55	55	55	55	55
[Fe/H] Loop no:	−2.014	−2.018	−2.022	−2.027	−2.031	−2.035
2	−2.014	−2.018	−2.023	−2.027	−2.032	−2.036
3	−2.013	−2.018	−2.023	−2.028	−2.033	−2.038
4	−2.010	−2.016	−2.023	−2.029	−2.035	−2.040
5	−2.005	−2.014	−2.022	−2.029	−2.037	−2.044
6	−1.997	−2.008	−2.019	−2.030	−2.040	−2.050
Mean	−2.009	−2.015	−2.022	−2.028	−2.035	−2.041
Sum σ^2 ($\times 10^{-6}$)	227	77	12	7	57	159